Vibrational Spectroscopy and ab Initio Calculations on $[N(C_2F_5SO_2)_2]^-$ and the Corresponding Superacid $HN(C_2F_5SO_2)_2$

Patrik Johansson,[†,‡] Jörgen Tegenfeldt,[‡] and Jan Lindgren*[,‡]

The Ångström Laboratory, Inorganic Chemistry, Uppsala University, Box 538, SE-751 21 Uppsala, Sweden

Received: June 8, 1999; In Final Form: October 18, 1999

A potential energy surface (PES) has been calculated for the PFSI anion, $[N(C_2F_5SO_2)_2]^-$, (bis(pentafluoroethanesulfone)imide ion), using quantum mechanical ab initio Hartree−Fock SCF molecular orbital methods (HF/6-31G*). Two different minimum energy structures have been found, and the vibrational spectra have been calculated for the two conformers. The energy difference between the two conformers is small, 5.4−7.3 kJ mol^{-1}, and the energy barrier between them is low, ∼2.3 kJ mol^{-1}, according to the PES. Thus, a large internal flexibility of the anion, a significant population of the two conformers, and rapid conversion between the two even at room temperature can be expected. Infrared vibrational spectra of the lithium salt of the anion, LiPFSI, dissolved in poly(ethylene oxide), PEO, have been recorded and compared with the calculated spectra, which suggest that no ion pairs of Li^+−PFSI are present for ether O/Li ratios $n > 6.5$. Comparisons are also made with ab initio calculations on the corresponding superacid HPFSI and with previously reported calculations and spectra on the more commonly used TFSI anion. The electronic structure of the PFSI anion and its calculated thermodynamic stability are evaluated from the point of view of the anion's use as a highly noncoordinating anion in solid polymer electrolytes in novel thin-film lithium polymer batteries (LPB's). No significant features that allow us to prefer PFSI to TFSI for usage in LPB's were found.

Introduction

Polymer-based thin-film all-solid-state battery concepts and materials suitable for usage in such devices are a globally intense research area.[1,2] In their most simple layout, such batteries use a polymer electrolyte as the ion conducting electrolyte made by dissolving an inorganic salt in a polymer matrix, often PEO, poly(ethylene oxide). In recent years several lithium salts with the general formula of $LiN(C_xF_ySO_2)_2$ have been synthesized and proposed as suitable components in such solid polymer electrolytes (SPE's) for usage in lithium polymer batteries (LPB's)[3]. The most used is the LiTFSI salt ($x = 1$, $y = 3$). Polymer electrolytes based on salts using the TFSI ion show on the average higher ion conductivity than any other anion, regardless of the cation used. This can be attributed to (a) the extremely delocalized negative charge of the TFSI anion,[3−5] which can be expected to be spread out over five atoms (the nitrogen atom and the four oxygen atoms), resulting in a highly noncoordinating ion, (b) the internal flexibility of the ion,[4] and (c) its bulkiness.[4,5] Much effort has been made to characterize these properties and to optimize SPE's based on the LiTFSI salt.[6,7]

Generally, the focus has been on the development and characterization of the electrodes and the electrolytes for LPB purposes. The characteristics of the current collectors have apparently been of less interest. However, by using electrochemical corrosion test techniques on an Al/LiTFSI$(PEO)_8$/Li cell, SPE's using the LiTFSI salt were recently found to cause pit corrosion in the aluminum current collector.[8] This kind of phenomenon was not unprecedented; Munshi et al.[9] had already reported corrosion behavior in a Li/Li$CF_3SO_3(PEO)_8/V_6O_{13}$ cell. For the battery behavior when it is overcharged and for the shelf life of the batteries, these reports may point to a severe technological problem. Thus, there is a need and scientific interest to find component replacements to avoid corrosion as well as to enhance or at least sustain the usually considered important properties (e.g., the ionic conductivity).

A possible solution is the exchange of either the salt or the current collector for a different material, preferably retaining lithium as the cation. Therefore, the search for a replacement has focused on the next anion in the $[N(C_xF_ySO_2)_2]^-$ series, the "beti" or "PFSI" anion (P for *penta*) having $y = 5$ and $x = 2$. A combined theoretical and experimental study on the PFSI anion and its corresponding acid, HPFSI, has therefore been undertaken. The main objective is not only to reveal the electronic structure of the anion and its vibrational spectra but also to predict possible differences in chemical stability compared to the TFSI anion.

By employing ab initio quantum mechanical calculations, we have earlier studied the PES (potential energy surface) of the TFSI anion for rotations about the central S−N bonds.[4] To provide the same data about the PFSI anion and to examine how replacing the CF_3 end groups by C_2F_5 affects the PES, a similar study is presented in the current paper. For the use of the PFSI anion as a component in SPE's it is clearly of interest to see if the electronic structure calculations can give information about its suitability as a replacement for/competitor to the TFSI anion.

One of the most common techniques for analysis of SPE's is vibrational spectroscopy. This is especially true for probing the occurrence of ion pairs or higher aggregates,[10−13] all of which lower the number of effective charge carriers in the SPE, and/or for detecting crystalline PEO or new crystalline phases

* To whom correspondence should be addressed. E-mail: Jan.Lindgren@kemi.uu.se.

[†] Present address: Chemistry Department, Northwestern University, 2145 Sheridan Rd, Evanston, IL 60208-3113.

[‡] Uppsala University.

10.1021/jp991866y CCC: $19.00
Published on Web 01/19/2000

in the simple salt/PEO blends.[14−16] In the present work, we report the vibrational spectra for the lithium salt of the PFSI anion, LiPFSI, dissolved in PEO and compare it to the calculated spectrum for the anion. The analysis both serves to assign the vibrational bands for the PFSI anion and as a fingerprint reference for SPE's based on the LiPFSI salt.

Experimental Section

The highly hygroscopic LiPFSI salt (a gift from 3M) was dried in a vacuum at 150 °C for more than 24 h. All subsequent handling of the dry salt was made in dryboxes filled with Ar or N_2. Solutions of $LiPFSIPEO_n$ (PEO from Aldrich, M_w = 4 000 000 Da; ether oxygen/lithium ratios n = 6.5, 9, 12, 16, 20, 40) were made by dissolving appropriate amounts of the components separately in CH_3CN (Merck, spectroscopic grade, dried with 4 Å molecular sieves) and then mixing them together quantitatively. Stirring was then allowed overnight.

The samples for the infrared (FT-IR) measurements were made by spreading the resulting solutions over a KRS-5 (TlI/TlBr) window and letting the secondary solvent slowly evaporate. The window was then mounted in a vacuum cell and heated to 50 °C under vacuum to remove any possible residual traces of water and CH_3CN. This was monitored in the OH stretching and the CN stretching regions in the infrared spectra, respectively. After slow cooling to room temperature (∼25 °C) spectra were recorded using 64 scans and a resolution of 2 cm^{-1}.

Samples of LiPFSI and LiTFSI (Aldrich, dried as LiPFSI) dissolved in PPG, poly(propylene glycol) (Aldrich, M_w = 3000 Da) were made as above for a fixed ether oxygen/lithium ratio of n = 10. The spectra were recorded using 256 scans and a resolution of 8 cm^{-1}. All spectra were recorded on a Digilab-Bio-Rad FTS-45 instrument.

Computational Methods

In an earlier paper[4] two stable structures of the TFSI anion were found by using ab initio Hartree−Fock (HF) self-consistent field (SCF) molecular orbital calculations by using the Gaussian 94 program[17] and the standard 6-31G* basis set. The two conformations of the TFSI anion from that paper were subsequently used mainly to investigate the vibrational assignments,[7] but the C_2 symmetry conformation was also used to locate the minimum energy geometry for the corresponding acid, the HTFSI molecule. In the present work, the same computational approach has been used for the PFSI anion (and the HPFSI acid) to enhance the direct comparison of results. Because it was previously found for the TFSI anion that extending the basis set to 6-31+G* did not produce any significant changes in geometry or relative energies, the computationally less expensive 6-31G* basis set was used for the PFSI anion.

A potential energy surface (PES) for the PFSI anion has been determined through rotations about the two central S−N bonds in a two-dimensional grid. The step size in the grid was 30°, and in each step all other parameters were fully optimized. A planar cis C−S−N−S dihedral angle is equal to 0°. A difference map between the PES for the PFSI and the PES for the TFSI was calculated within the grid values {60°, 60° − 300°, 300°}: $\Delta E_{DIFF} = \Delta E_{PFSI} - \Delta E_{TFSI}$.

The local minimum energy structures obtained from the PES grid were subsequently fully optimized employing the same basis set. The geometry of the HPFSI acid was calculated at the HF/6-31G** level using geometry information from the obtained C_2 PFSI structure and the HTFSI structure from ref 7 to generate starting values. Single-point energy calculations were performed to assess the accuracy of the energy difference between the two unique minima found for the PFSI anion, employing larger basis sets and using different levels of theory.

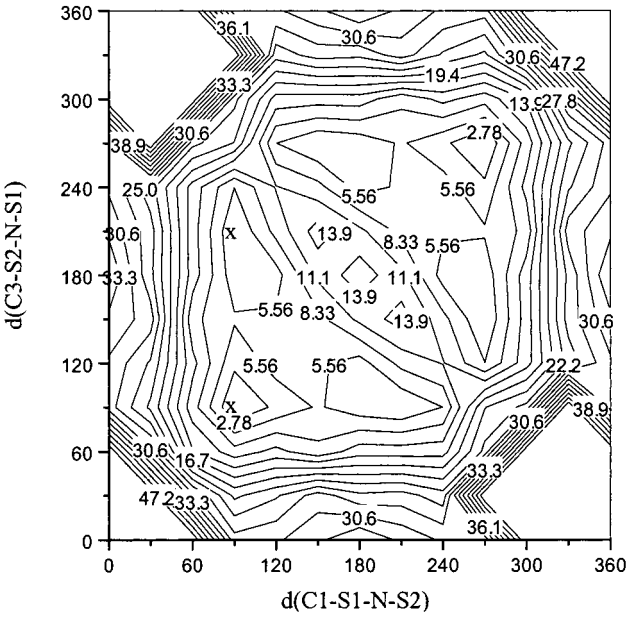

Figure 1. PES for the PFSI anion calculated at HF/6-31G*. The two unique local minima found are marked with "x".

The vibrational frequencies, IR intensities, and Raman activities were calculated for all fully optimized structures to confirm them as true energy minima structures and for experimental comparison purposes. The potential energy distribution (PED) matrix for both conformations of the anion was calculated with the GAMESS program.[24] The Spartan program[25] was used to visualize the vibrational modes to assist in the assignment of the spectra. The assignments, however, are based mainly on the PED, since many modes are too complex to be described unambiguously in terms of group vibrations, as detected by viewing the modes.

The thermodynamic stability of the anion was evaluated using the concept of chemical hardness (η). By applying Koopman's theorem, Pearson showed[18,19] that 2η is equal to the gap between the HOMO and LUMO levels (for closed-shell molecules). It is now generally agreed that an increase in the HOMO−LUMO gap is linked to the thermodynamic stability of a species.[20−23] In the present study, the HOMO−LUMO gap was calculated for a set of anions often used in SPE's. This was done both at the level of geometry optimization (HF/6-31G*) and at the HF/6-311+G**//HF/6-31G* level.

Results and Discussion

PFSI Anion. *Potential Energy Surface*. The calculated PES for the PFSI anion is shown in Figure 1. From this PES, two unique local minima with a low energy difference between them were detected. The nature of the former will be discussed in more detail in the geometries and energies section below. Furthermore, the PES also reflects the possibility of conversion between the two conformers with a low cost in potential energy; the barrier estimated from the PES is only 2.3 kJ mol^{-1} via the lowest energy path. Dynamic conversion between the obtained stable structures as well as a significant population of both conformers can thus be expected, even at room temperature. The relative population of each conformer should be temperature-dependent.

The PES has a central area with both the C−S−N−S dihedral angles within 60°−270° where the relative energy difference

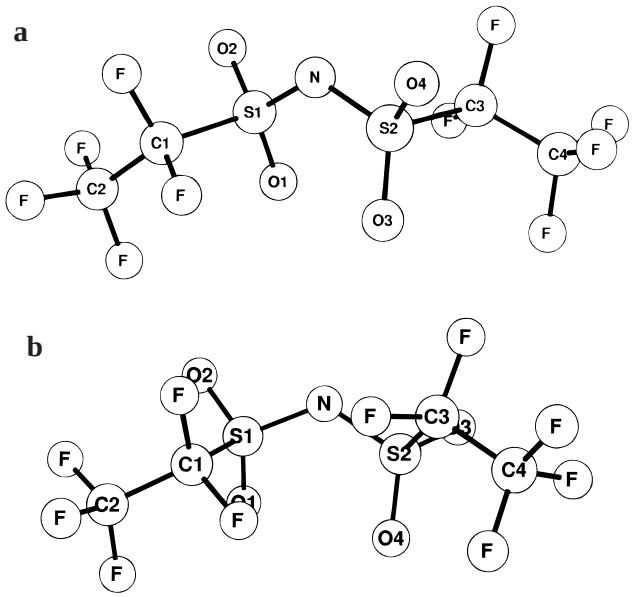

Figure 2. (a) C_2 symmetry global minimum energy structure. (b) C_1 symmetry local minimum energy structure.

does not exceed 22 kJ mol^{-1}. The outer parts of the PES (striped in Figure 1) have not been possible to calculate; no SCF convergence was achieved and/or in some cases steric hindrances occurred. However, these areas are behind large barriers, the calculated points next to them having large relative energy values, and would thus be of less importance and interest. The "real" PES would possibly be drastically different if the anion interaction with the surrounding media was strong, but this is not the prime case for "good" anions in SPE systems in general.[26] Therefore, a calculated PES for an anion in a vacuum is a handy tool for detecting the stable structure(s) as well as interpreting the flexibility of the anion in such systems.[4,27]

Geometries and Energies. The two unique local minima at grid points (90, 90) and (90, 210) in the obtained PES, with a relative energy difference of only 6.2 kJ mol^{-1}, were used as starting points for full geometry optimizations at the HF/6-31G* level. The two resulting minimum energy geometries are depicted in Figure 2. Selected geometry parameters are listed in Table 1, together with the data for the TFSI anion from ref 4, the HPFSI acid data from this study, and the HTFSI acid data from ref 7. The lower energy conformation, the global minimum (Figure 2a), has C_2 symmetry, whereas the other (Figure 2b) has C_1 symmetry. The energy difference between the two conformers is only 5.6 kJ mol^{-1} (HF/6-31G*; Table 2).

To improve the accuracy in the evaluation of the energy difference, single-point calculations were performed employing a larger basis set and/or other levels of theory (Table 2). From these data, the HF/6-31G* basis set seems to give an accurate value for the energy difference: within 1.7 kJ mol^{-1} relative to the more sophisticated and CPU-time-demanding methods, including the post-HF methods. Even when the geometry of the anion was optimized using methods including electron correlation (DFT-B3LYP/6-31G*), the energy difference remained in that interval.

To the best of our knowledge, there exists no experimental structure determination comprising the PFSI anion entity. For the TFSI anion, on the other hand, several structure determinations of different salts have been reported.[27,28] Therefore, the structural results for the PFSI anion will primarily be compared with the TFSI structure from these reports and with earlier calculations on the TFSI anion.[4,29]

Comparison with TFSI. From this study performed to facilitate comparison with the TFSI anion, several direct comparisons of relevance can be made. The obtained C_2 symmetry conformers of the two anions have almost identical geometries for the central parts (Table 1). The central S−N−S angles show just a 0.1° difference and the C−S−N−S dihedrals only a 0.7° increase for the PFSI. Both changes are thus on the subpercentage level. All changes in bond lengths are less than 0.003 Å except for the C−S bonds that differ by 0.012 Å. This may be due to the stronger electron-withdrawing power of the C_2F_5 entity compared to CF_3, leaving the C−S bonds weakened.

In an earlier calculation on the TFSI anion Benrabah et al.[29] reported a C_2 symmetry structure with an S−N−S angle of 156°, clearly larger than the present results. However, their calculations were made using the 3-21+G* basis set and their value also clearly differs from that obtained from the crystal structure (125°). In ref 4 it was found that a large change in the S−N−S angle might lead to significant changes in the charge distribution in the anion. Differences up to 40% were reported. Therefore, even if employing a smaller basis set may seem tempting as the anion size increases (as in the present case), it is not always a fruitful way.

The obtained C_1 symmetry conformers show larger differences. The central dihedral angles (C−S−N−S) are 89.6° and −134.5° for PFSI compared to 99.8° and −168.2° for the C_1 conformer of TFSI. These changes are on the 10−20% level. The reason for this may be found in the calculated PES's. For PFSI as well as for TFSI[4] the PES is flatter in the vicinity of the C_1 conformer minimum than near the minimum corresponding to the C_2 conformer. Small differences in the PES's in the former region may thus lead to large changes in the stable geometries for the C_1 symmetry conformers of the two anions. A difference map between the two PES's (ΔE_{DIFF}) is shown in Figure 3. The obtained calculated changes are, however, quite small, the only major change being the higher relative value for the central part of the map, where both anions have their maximum extension in space. The C_1 conformer region changes are too small to be detectable by eye. This further emphasizes both the similarity between the flexibility of the two anions and how only subtle changes in the PES may result in large differences in the obtained stable geometries.

Charge Distribution. In Table 3 the Mulliken charges for the two conformers of the anion and the HPFSI acid are listed. The atomic charges for the two anion conformers are almost the same. Thus, the large changes in the C−S−N−S dihedral angles do not seem to cause severe charge redistribution within the anion. However, compared to the TFSI anion,[4] replacing CF_3 by C_2F_5 influences primarily the carbon atoms (C1, C3) attached to the sulfur atoms: a ∼0.4 charge decrease for each one of the two atoms is observed for both conformers. However, the sum of atomic charges for C_2F_5 is −0.24, and for CF_3 it is −0.20. The implication of this charge difference for the C−S bonds has been discussed above, and it may also affect the vibrational modes with contributions from the C−S coordinates.

For both PFSI conformers, as for TFSI, the largest negative charge is found on the nitrogen atom (−0.94). This is in agreement with the fact that the proton is residing on the nitrogen atom in the HTFSI acid.[28] Also, considerable negative charge is found on the oxygen atoms. From the ion-pairing point of view, Li^+−PFSI ion pairs being especially important, the possible coordination to different atoms in the PFSI ion should

TABLE 1: Selected Geometry Parameters for the Two Conformers of the PFSI Anion and for the HPFSI Acid[a]

	C_2 symmetry			C_1 symmetry			C_2 symmetry acid	
	PFSI HF/6-31G*	PFSI B3LYP/6-31G*	TFSI[4] HF/6-31G*	PFSI HF/6-31G*	PFSI B3LYP/6-31G*	TFSI[4] HF/6-31G*	HPFSI HF/6-31G*	HTFSI[7] HF/6-31G*
r(C−F) (av CF_3)	1.315	1.339	1.315	1.315	1.343	1.315	1.308	1.303
r(C−F) (av CF_2)	1.328	1.353		1.329	1.354		1.320	
r(C1−C2)	1.533	1.544		1.533	1.544		1.536	
r(C3−C4)	1.533	1.544		1.534	1.545		1.536	
r(S1−C1)	1.832	1.889	1.820	1.832	1.887	1.820	1.831	1.825
r(S2−C3)	1.832	1.889	1.820	1.830	1.888	1.817	1.831	1.825
r(S1−O1)	1.429	1.466	1.430	1.429	1.466	1.430	1.410	1.411
r(S1−O2)	1.431	1.470	1.431	1.431	1.469	1.433	1.415	1.416
r(S2−O3)	1.431	1.470	1.431	1.430	1.468	1.432	1.415	1.416
r(S2−O4)	1.429	1.466	1.430	1.431	1.470	1.434	1.410	1.411
r(S1−N)	1.573	1.619	1.575	1.566	1.612	1.569	1.659	1.660
r(S2−N)	1.573		1.575	1.575	1.619	1.579	1.659	1.660
r(N−H)							1.003	1.003
a(O1−S1−O2)	118.4	119.0	118.5	118.6	119.2	119.0	123.9	124.0
a(O3−S2−O4)	118.4	119.0	118.5	118.1	118.8	117.8	123.9	124.0
a(O1−S1−N)	109.3	108.1	109.2	109.3	107.6	110.2	109.9	109.6
a(O2−S1−N)	116.3	117.2	116.0	115.2	116.1	114.7	105.0	104.9
a(O3−S2−N)	116.3	117.2	116.0	111.9	110.2	114.2	105.0	104.9
a(O4−S2−N)	109.3	108.1	109.2	116.3	117.5	115.1	109.9	109.6
a(C1−S1−N)	102.0	101.7	102.9	103.8	104.8	103.4	100.7	102.2
a(C3−S2−N)	102.0	101.7	102.9	98.5	98.8	97.1	100.7	102.2
a(S1−N−S2)	127.9	124.0	127.8	128.2	125.4	125.6	130.7	130.5
a(H−N−S)							114.6	114.8
d(O1−S1−N−S2)	−156.9	−160.2	−157.9	−160.6	−168.1	−150.7	−158.1	−160.7
d(O2−S1−N−S2)	−19.6	−22.3	−20.7	−24.1	−31.6	−13.0	−22.8	−25.6
d(O3−S2−N−S1)	−19.6	−22.3	−20.7	116.4	128.6	82.4	−22.8	−25.6
d(O4−S2−N−S1)	−156.9	−160.2	−157.9	−23.5	−11.8	−58.9	−158.1	−160.7
d(C1−S1−N−S2)	93.4	90.6	92.7	89.6	82.4	99.8	90.9	88.6
d(C3−S2−N−S1)	93.4	90.6	92.7	−134.5	−123.3	−168.2	90.9	88.6
d(C2−C1−S1−N)	−171.7	−166.7		−176.3	−176.9		−175.3	
d(C4−C3−S2−N)	−171.7	−166.7		176.7	168.6		−175.3	
d(C−S−N−H)							−89.1	−91.4

[a] Bond lengths (r) in Å and bond angles (a, d) in degrees.

TABLE 2: Total and Relative Energies for the Two PFSI Anion Conformers at Different Levels of Calculation

method	energy (au)		ΔE (kJ mol^{-1})
	PFSI, C_2	PFSI, C_1	
HF/6-31G*//HF/6-31G*	−2 294.674 195	−2 294.672 052	5.6
HF/6-311+G**//HF/6-31G*	−2 295.141 314	−2 295.139 249	5.4
MP2/6-31G*//HF/6-31G*	−2 298.036 509	−2 298.034 212	6.0
B3LYP/6-31G*//HF/6-31G*	−2 302.751 221	−2 302.748 442	7.3
B3LYP/6-31G*//B3LYP/6-31G*	−2 302.769 861	−2 302.767 607	5.9
B3LYP/6-311+G**//HF/6-31G*	−2 303.311 114	−2 303.308 849	5.9
B3LYP/6-311+G**//B3LYP/6-31G*	−2 303.327 094	−2 303.324 507	6.8

be considered, mainly to the nitrogen atom and to the oxygen atoms, but perhaps also additional coordination by the fluorine atoms.

Vibrational Frequencies. The experimental (FT-IR) spectra for $LiPFSIPEO_n$ (n = 6.5, 9, 12, 16, 20, 40) in the range 400−1400 cm^{-1} are shown in Figure 4. The calculated (for the C_2 conformer) and observed infrared vibrational frequencies (from Figure 4, n = 9) for the PFSI ion are compared in Table 4. Ion-pairing in SPE systems has earlier been shown to be important for low values of n, high salt concentrations.[10−13] On the other hand, for high values of n there may be regions of crystalline PEO in the samples.[14−16] Since the measurements are made at room temperature, the occurrence of crystalline regions will strongly influence the spectra. This is also true for the room temperature ion conductivity, which takes place predominantly in the amorphous regions, as first shown by NMR measurements,[30] and therefore will be lower in such samples.

All fundamental vibrations of the PFSI ion can be found below 1400 cm^{-1}, and therefore, the analysis of the spectra is restricted to the region 400−1400 cm^{-1}. Furthermore, the spectra should be rather similar to the spectra from $LiTFSIPEO_n$ samples,[7] with some additional features. The samples with the low salt content (n = 16, 20, 40) show a strong absorption band at ∼1110 cm^{-1}. This peak has earlier been assigned to arise from crystalline PEO, a vibrational mode with contributions mainly from C−O−C stretching in the polymer backbone.[14−16] According to the discussion above, these samples will not be of main interest.

On the other hand, the sample with the highest salt content (n = 6.5) shows new bands arising at 1190 and 1120 cm^{-1} and in addition a shoulder at 1058 cm^{-1}. A new crystalline phase or at least short-range order in the sample could be responsible for these features. Vallee et al. established the phase diagram for $LiTFSIPEO_n$, in which there is a crystalline phase for n = 6.[6] The shoulder at 1058 cm^{-1} is also present at a slightly higher wavenumber (1060 cm^{-1}) for the n = 16, 20, and 40 samples. Whether or not this shoulder could be attributed to ion-pair formation is certainly a relevant issue. A recent study on gel electrolytes containing LiTFSI indicates that no contact ion pairs are formed for 0.5 and 1 M solutions, whereas an increase in

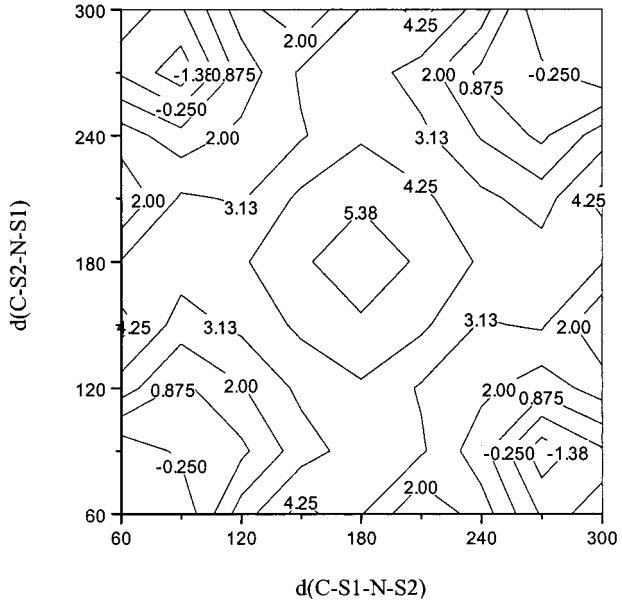

Figure 3. Difference map between the PES's for PFSI and TFSI.

TABLE 3: Mulliken Charges for the Two Conformers of the PFSI Anion and the HPFSI Acid

atom	PFSI, C_2	PFSI, C_1	HPFSI, C_2
H			0.40
N	−0.94	−0.94	−1.01
S1	1.57	1.57	1.63
S2	1.57	1.57	1.63
O1	−0.66	−0.67	−0.61
O2	−0.69	−0.68	−0.60
O3	−0.69	−0.66	−0.60
O4	−0.66	−0.68	−0.61
C1	0.46	0.45	0.47
C2	1.07	1.07	1.09
C3	0.46	0.47	0.47
C4	1.07	1.07	1.09
F (av CF_2)	−0.36	−0.36	−0.34
F (av CF_3)	−0.35	−0.35	−0.33

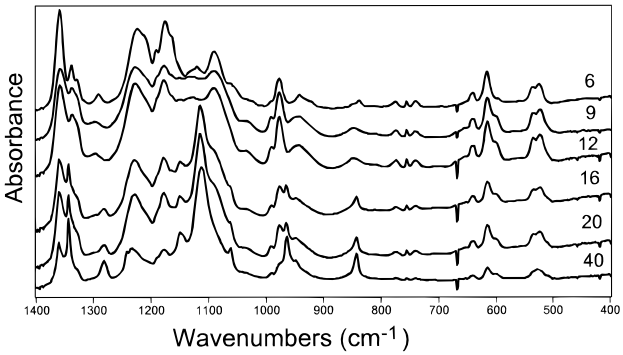

Figure 4. FT-IR spectra for $LiPFSIPEO_n$ at 25 °C.

concentration to ∼5 M shows clear evidence of substantial ion-pairing.[31] Therefore, ion-pairing in the high O/Li ratio samples seems less likely, and the band at 1060 cm^{-1} should not arise from such species. However, the shoulder at 1058 cm^{-1} for $n = 6.5$ (∼4 M) could contain a contribution from cation−anion interaction, but severe overlap with the bands from the PEO makes any quantitative comparison ambiguous.

The spectra for $n = 9$ and 12 are very similar to each other; no features from crystalline PEO are present and no ion-pairing seems to occur. However, ion-pairing in general has been shown to increase with temperature. The room-temperature spectra can thus be treated in conjunction and can be compared with the spectra of $LiTFSIPEO_8$ from ref 7. Even if there are no bands arising from crystalline PEO for these samples, the bands from amorphous PEO interfere with our analysis. Therefore, by comparison with earlier studies, we will focus on specific regions of interest. The B modes will be of main interest because they are more intense in IR spectra. The A modes are more Raman active.

First, the stretching vibrations of the SO_2, CF_3, and CF_2 groups occur in the region 1500−1000 cm^{-1}. By comparison with earlier data, we assign the band centered at 1357 cm^{-1} (calculated at 1343) to $\nu_a(SO_2)$ (in-phase) and the lower, less intense band of B symmetry at 1337 cm^{-1} (1320) to $\nu_a(SO_2)$ (out-of-phase). This is clearly also in agreement with the calculated intensity relationships. Between 1300 and 1000 cm^{-1} some features emerge. The spectra have maxima at ∼1177 cm^{-1} and a second peak at ∼1225 cm^{-1}, and these are assigned to mixed modes of $\nu_s(SO_2)$, $\nu_s(CF_2)$, and $\nu_a(CF_3)$. For TFSI a band is present at ∼1060 cm^{-1}; we observe a band at 1084 cm^{-1} (1088). This band has been assigned as ν_a(SNS) for TFSI. The upshift is ∼24 cm^{-1}. However, PEO, when complexed with a cation, has a ν(COC) vibration at just about 1080 cm^{-1}, and therefore, any precise shift determinations are impossible. Interestingly, the corresponding shift in the calculated values is 26 cm^{-1}.

Furthermore, a band is calculated at 1016 cm^{-1}, seemingly having no counterpart neither for TFSI nor in the experimental spectra. In the experimental spectra there is, however, a continuous growth of a band at ∼976 cm^{-1} with increasing salt concentration. From the PED this band is a very mixed mode with main contributions from CF_3 stretching coordinates. The C−S stretching contribution may explain why there is no counterpart in the TFSI case, the C−S bond being weakened in the PFSI.

The next bands observed are well-known from the TFSI anion: a triplet of bands at 741 cm^{-1} (calculated at 737), 754 cm^{-1} (758), and 773 cm^{-1} (771). Corresponding values for TFSI are 739 cm^{-1} (733), 761 cm^{-1} (767), and 788 cm^{-1} (786). The intense Raman band at ∼740 cm^{-1} has been used to probe ion-pairing in SPE systems, and the mode has almost always been assigned as $\delta_s(CF_3)$. However, in the PED for TFSI no major contribution from F−C−F coordinates was found.[7] Visualizing the vibration, both for TFSI and for PFSI, gives a mode where the whole anion expands and contracts. Such behavior should give high Raman activity, in agreement with the observations from experiment. Furthermore, the calculations reveal a higher intensity for PFSI compared to TFSI, increasing with 18% in Raman activity and 78% in IR intensity. If the vibration were due to a $\delta(CF_3)$ mode, this behavior would not be explained, the number of oscillators being the same in both anions. On the other hand, if all atoms were to contribute to this mode, it would be easier to explain. Thus, the present work strongly supports the ν_s(SNS) assignment of the ∼740 cm^{-1} band,[7] but it should rather be called an "expansion/contraction" mode.

Moreover, the whole concept of using CF_3 units is perhaps misleading. Visualization of the two higher modes of the band triplet and the mode calculated at 1016 cm^{-1} shows decoupling of the three C−F bonds in each CF_3 entity. This may be due to lack of symmetry; approximate C_3 axes should not be considered but rather approximate mirror planes at the end of the anions. This was suggested also for the TFSI anion.[7]

Thermodynamic Stability and Chemical Hardness. Even if the HOMO and LUMO levels for a chemical entity strictly speaking are only just mathematical conveniences and not physical observables, they can be used in several qualitative

TABLE 4: Selected Vibrational Frequencies, Infrared Intensities, and Raman Activities for the C_2 Conformer of the PFSI Ion

ν (cm^{-1})						
unscaled	scaled (×0.91)	observed	IR intensity (km mol^{-1})	Raman active (A^4 amu^{-1})	mode (% of PED)	symmetry
569	517	523	162.6	0.7	N−S−O (65)	B
587	534	534	55.6	0.4	F3−C−C−S (43); F2−C−S−N (16); N−S−O (10)	B
653	594	601	3.6	1.0	F3−C−C−S (48); C−F3 (17); C−C−S−N (12)	B
698	635	615	336.6	0.4	O−S−N−S (57); N−S−O (18); F3−C−C−S (10)	B
700	637		2.2	4.1	O−S−N−S (23); N−S−O (23); F2−C−S−N (16)	A
711	647	641	198.6	0.4	F2−C−S−N (22); F3−C−C (17); C−F2 (15); C−S−N (12)	B
810	737	741	58.0	19.7	S−N (29); N−S−O (16); F3−C−C (16); C−F3 (15)	A
833	758	754	10.8	0.1	C−F3 (41); F3−C−C (30)	B
847	771	773	8.8	1.0	C−F3 (29); S−N (23); F3−C−C (15); N−S−O (13)	A
1116	1016	976	269.5	0.0	C−F3 (30); F2−C−S (18); C−S (14); S−O (10)	B
1195	1088	1084	233.6	0.0	S−N (37); S−O (36); C−F2 (13)	B
1264	1150		44.5	11.6	S−O (77); C−F2 (11); S−O (5)	A
1275	1160	1177	689.4	0.3	S−O (49); S−N (39)	B
1340	1220		81.0	4.9	C−F2 (43); C−F3 (19); C−S (12)	A
1345	1224	1227	315.3	0.4	C−F2 (51); C−F3 (10); C−S (10)	B
1353	1231		104.3	1.5	C−F2 (83)	A
1359	1237		385.5	0.5	C−F2 (75); S−N (6)	B
1395	1270		458.8	0.1	C−F3 (80); F−C−C−S (15)	B
1397	1271		24.1	10.7	C−F3 (55); F−C−C−S (15)	A
1421	1293		69.2	0.4	C−F3 (59); S−O (26)	B
1424	1296		76.4	0.7	C−F3 (63); S−O (13); F−C−C−S (10)	A
1451	1320	1337	293.6	3.2	S−O (69); C−F3 (24)	B
1476	1343	1357	827.8	2.2	S−O (81); C−F3 (10)	A
1528	1390		160.8	2	C−C (41); C−F3 (22); F3−C−C (18); C−F2 (10)	B
1533	1395		44.1	3.5	C−C (41); C−F3 (22); F3−C−C (18); C−F2 (11)	A

TABLE 5: Thermodynamic Stability of Some Anions Commonly Used in SPE's, Including PFSI

anion	ϵ_{HOMO}[a] (eV)	ϵ_{LUMO}[a] (eV)	η[a] (eV)
PFSI, C_2	−8.24	8.51	8.38
	−8.59	**4.58**	**6.58**
PFSI, C_1	−8.08	8.94	8.51
	−8.46	**4.51**	**6.48**
TFSI, C_2	−8.06	9.64	8.85
	−8.41	**4.78**	**6.59**
TFSI, C_1	−7.78	9.88	8.83
	−8.16	**4.74**	**6.45**
AsF_6^-	−11.14	11.42	11.28
	−11.97	**5.61**	**8.79**
PF_6^-	−10.72	14.08	12.40
	−11.46	**5.57**	**8.51**
BF_4^-	−9.55	17.17	13.36
	−10.35	**5.98**	**8.17**
ClO_4^-	−7.21	13.98	10.59
	−7.67	**6.69**	**7.18**
$CF_3SO_3^-$	−6.84	12.77	9.81
	−7.30	**5.33**	**6.31**
Cl^-	−3.39	22.31	12.85
	−4.08	**8.16**	**6.12**

[a] Light-faced values are calculated using HF/6-31G*, and bold-faced values are calculated using HF/6-311+G**//HF/6-31G*.

descriptions of chemical and physical properties. Calculated HOMO and LUMO energy levels are listed in Table 5 not only for the two PFSI conformers but also for a set of the most commonly used anions in SPE studies. As previously compared by Benrabah et al. for the triflate, TFSI, and the "methide" anions,[29] we compare the gap between the HOMO and LUMO levels for the different anions, a difference that is linked to the thermodynamic stability using the concept of chemical hardness (η).[18−23]

One way of comparing the calculated hardness with an experimental quantity is to use the shift in the OH stretching frequency for a molecule containing an OH group, which can be hydrogen-bonded to an anion. In this way, the anions can be classified according to their hydrogen bond acceptor strength, which is dependent mainly on their polarizability, and this in turn is closely linked to their hardness. The polarizability can be expected to decrease if the ionic charge is distributed among several centers of a polyatomic ion (e.g., PFSI), and similarly, the hardness increases. The harder the anion the smaller is the OH frequency shift and the acceptor strength. OH stretching frequency shifts have earlier been used to classify organic solvents according to their basicity.[32] In the present case where we have a hydrogen bond to a charged ion, where the interaction is dominated by an ion−dipole interaction, we restrict our comparison mainly to monovalent anions containing oxygen or fluorine as the acceptor atoms. This is done in order to avoid any large variations in atomic size that would complicate the comparison.

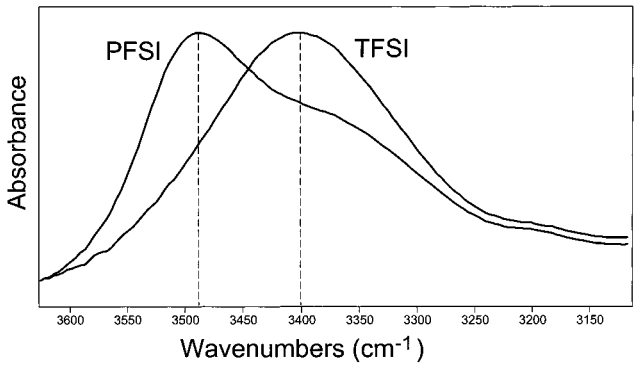

Figure 5. FT-IR spectra for $LiPFSIPPO_{10}$ and $LiTFSIPPO_{10}$ at 25 °C.

Bernson et al. used the observed infrared bands in the OH stretching region of $LiX(PPG)_{10}$ samples (for X = PF_6^-, BF_4^-, ClO_4^-, $CF_3SO_3^-$, I^-, and Br^-) to evaluate the hydrogen bond acceptor strength.[33] PPG, poly(propylene glycol), with the repeat unit [−CH_2−CH(CH_3)−O−], is fully amorphous at room temperature when the different lithium salts are also dissolved into the polymer matrix. For $LiTFSI(PPG)_{10}$ the OH stretching band is observed at 3400 cm^{-1} and for $LiPFSI(PPG)_{10}$ at 3490 cm^{-1} (Figure 5). Included in the experimental series below is also the band arising from coordination of ether oxygen (EO) from the PPG polymer backbone to the OH end groups. The

sequence of observed infrared bands is

$$AsF_6^- \sim PF_6^- > BF_4^- \sim PFSI > ClO_4^- \sim TFSI > EO \sim CF_3SO_3^- > Cl^-$$

The calculated order of chemical hardness (from the HOMO and LUMO values) from the HF/6-31G* calculations is

$$BF_4^- > Cl^- > PF_6^- > AsF_6^- > ClO_4^- > CF_3SO_3^- > TFSI > PFSI \text{ (Table 5)}$$

The calculated order of chemical hardness is clearly not in good agreement with the experimental study. Furthermore, deviation from general chemistry knowledge does occur; the HTFSI acid is known to be a stronger acid than the triflic acid (CF_3SO_3H). Therefore, the order of their anions should be reversed, and in this selection of anions the chloride ion should be the strongest base. Improvements must clearly be made. Since the HOMO and especially the LUMO levels are highly sensitive to the basis set used in the calculations,[34] the significantly larger 6-311+G** basis set was employed to get a more accurate description of the MO's. The calculated series then becomes

$$AsF_6^- > PF_6^- > BF_4^- > ClO_4^- > PFSI \sim TFSI > CF_3SO_3^- > Cl^- \text{ (Table 5)}$$

This is clearly in considerably better agreement with the experimental order.

The order of the anions according to the strength of the hydrogen bond, as measured by the OH stretching shifts, is expected to be the same as for the interaction between Li and X, where X is an anion. The greatest tendency for ion-pair formation is thus found for Cl^- and $CF_3SO_3^-$. In this respect, we found no difference between TFSI and PFSI. If we compare the stability vs oxidation, using the calculated HOMO level values (Table 5), the PFSI anion is only *marginally less* stable than the TFSI anion. Thus, the present calculations of thermodynamic stability do not show any indication that supports LiPFSI as a suitable replacement for the LiTFSI salt owing to the anion being less corrosive to the Al current collector. However, it is not only the thermodynamic stability that determines this suitability.

HPFSI Acid. *Geometry and Charge Distributio*n. In Table 1 selected calculated geometry parameters for the HPFSI acid are listed (HF/6-31G**). Since no crystal structure determination exists, we will mainly compare with the HTFSI and the PFSI. The changes relative to the calculated values for HTFSI are small; the largest changes are for the C−S bonds, which follow the trend for PFSI/TFSI. The major changes compared to TFSI are the significantly shorter S−O bonds and longer S−N bonds. For TFSI/HTFSI, this was explained as due to less double-bond character for the S−N bonds upon protonation at the nitrogen.[7] The charge distribution is almost exactly as for HTFSI for the central part of the molecule. Upon protonation, electrons are transferred to the nitrogen, which increases its negative charge.

Vibrational Frequencies. No direct comparison with an experimental spectrum for the HPFSI acid can be carried out, since no such spectrum has been recorded. Therefore, the vibrational analysis will be conducted on the basis of several other comparisons: (a) with the PFSI anion, (b) with the calculations, and (c) with the spectrum for HTFSI (Table 6). The main purpose is to see if some of the features observed for the TFSI/HTFSI couple are still present and can be further substantiated.

TABLE 6: Selected Vibrational Frequencies, Infrared Intensities, and Raman Activities for HPFSI Acid

ν (cm^{-1}) unscaled	ν (cm^{-1}) scaled ($\times 0.91$)	IR intensity (km mol^{-1})	Raman active (A^4 amu^{-1})	symmetry	ν (cm^{-1}) calcd HTFSI[7] ($\times 0.90$)
555	505	176.6	0.7	B	498
578	526	0.0	2.0	A	
586	533	69.1	0.3	B	565
616	561	6.2	1.2	A	
651	592	5.5	1.4	A	
653	594	1.1	1.4	B	
689	627	11.4	1.6	A	
690	628	441.6	0.0	B	623
713	649	66.2	0.5	B	
715	651	1.5	1.6	A	
834	759	16.4	17.1	A	765
838	763	21.1	0.1	B	779
884	796	25.2	3.0	A	817
976	888	589.2	1.1	B	882
1129	1027	128.2	0.3	B	
1134	1031	15.45	2.7	A	
1276	1161	477.7	0.8	B	1126
1278	1163	61.9	9.9	A	1132
1329	1209	77.8	0.2	B	1244
1341	1220	42.8	9.1	A	1260
1393	1268	147.9	1.2	A	1289
1394	1269	110.7	0.5	B	1290
1436	1307	516.6	0.3	B	1306
1437	1308	2.2	6.7	A	
1443	1313	96.3	0.1	B	
1444	1314	285.3	1.8	A	
1483	1350	27.9	2.4	B	1335
1525	1388	258.1	2.6	B	
1531	1393	10.9	4.6	A	
1567	1426	606.5	1.5	A	1409
1582	1440	220.4	1.2	B	1422
3788	3447	166.2	35.8	A	3410

From comparison with the PFSI anion, one distinct difference can be observed: the band calculated at 1084 cm^{-1} has no counterpart for the acid. This phenomenon was observed also for TFSI/HTFSI and explained by the disappearing double-bond character for the S−N bonds upon protonation. The mode, denoted mainly as a ν_a(SNS) mode, then becomes downshifted $\sim$200 cm^{-1} to 888 cm^{-1}, which is a band without any counterpart in the spectrum for the PFSI anion. A weakening of the S−N bonds can of course also affect other bonds, and the S−O bonds do get stronger. The two $\nu_a(SO_2)$ bands are most affected with upshifts of $\sim$90 cm^{-1} to 1426 and 1440 cm^{-1}, respectively.

The strongest Raman band, apart from the N−H stretching band at 3447 cm^{-1}, is the band calculated at 759 cm^{-1}. Compared to the PFSI anion (the band at 741 cm^{-1}, calculated at 737) there is a shift of $\sim$20 cm^{-1}. If the mode is a $\delta(CF_3)$ mode, there is no obvious reason for a shift due to protonation at the nitrogen atom. On the other hand, for a ν_s(SNS) mode, the change is surprisingly small.

Conclusions

The PFSI anion is very similar to the TFSI anion in most aspects. The flexibility is high and the stable geometry sensitive to the PES, which proves to be important for the C_1 symmetry local minimum energy geometry. There is no evidence for the LiPFSI salt being more suitable in SPE's. The observed and calculated spectra further support the assignments for the TFSI and PFSI anions, especially important for the debated $\sim$740 cm^{-1} band used for ion-pair quantification. No contact Li^+−PFSI ion pairs seem to be present for the $n = 9$ and 12 concentrations of $LiPFSIPEO_n$.

Acknowledgment. This work was supported by computing resources from the Swedish Council for High Performance Computing (HPDR) and the Centre for Parallel Computers (PDC), Royal Institute of Technology (KTH), and by grants from the Swedish Natural Science Research Council (NFR).

References and Notes

(1) Scrosati, B. *Nature* **1995**, *373*, 557.
(2) Baril, D.; Machete, C.; Armand, M. *Solid State Ionics* **1997**, *94*, 35.
(3) Hu, L. Q.; DesMarteau, D. D. *Inorg. Chem.* **1993**, *32*, 5007.
(4) Johansson, P.; Gejji, S. P.; Tegenfeldt, J.; Lindgren, J. *Electrochim. Acta* **1998**, *43*, 1375.
(5) Foropoulos, J.; DesMarteau, D. D. *Inorg. Chem.* **1984**, *23*, 3720.
(6) Vallée, A.; Besner, S.; Prud'homme, J. *Electrochim. Acta* **1992**, *37*, 1579.
(7) Rey, I.; Johansson, P.; Lindgren, J.; Lassègues, J. C.; Grondin, J.; Servant, L. *J. Phys. Chem. A* **1998**, *102*, 3249.
(8) Chen, Y.; Devine, T. M.; Evans, J. W. *Electrochem. Soc. Proc.* **1997**, *96*−*17*, 187.
(9) Munshi, M. Z. A.; Gopalienger, R.; Owens, B. B. *Solid State Ionics* **1988**, *27*, 259.
(10) Papke, B. L.; Dupon, R.; Ratner, M. A.; Shriver, D. F. *Solid State Ionics* **1981**, *5*, 685.
(11) Dupon, R.; Papke, B. L.; Ratner, M. A.; Whitmore, D. H.; Shriver, D. F. *J. Am. Chem. Soc.* **1982**, *104*, 6247.
(12) Schantz, S.; Sandahl, J.; Börjesson, L.; Torell, L. M.; Stevens, J. R. *Solid State Ionics* **1988**, *28*−*30*, 1047.
(13) Bernson, A.; Lindgren, J. *Solid State Ionics* **1993**, *60*, 37.
(14) Bernson, A.; Lindgren, J.; Huang, W.; Frech, R. *Polymer* **1995**, *36*, 4471.
(15) Yoshihara, T.; Tadokoro, H.; Murimashi, S. *J. Chem. Phys*. **1964**, *41*, 2902.
(16) Matsuura, H.; Fukuhara, K. *J. Polym. Sci., Part B: Polym. Phys.* **1986**, *24*, 1383.
(17) Frisch, M. J.; Trucks, G. W.; Schlegel, H. B.; Gill, P. M. W.; Johnson, B. G.; Robb, M. A.; Cheeseman, J. R.; Keith, T.; Petersson, G. A.; Montgomery, J. A.; Raghavachari, K.; Al-Laham, M. A.; Zakrzewski, V. G.; Ortiz, J. V.; Foresman, J. B.; Cioslowski, J.; Stefanov, B. B.; Nanayakkara, A.; Challacombe, M.; Peng, C. Y.; Ayala, P. Y.; Chen, W.; Wong, M. W.; Andres, J. L.; Replogle, E. S.; Gomperts, R.; Martin, R. L.; Fox, D. J.; Binkley, J. S.; Defrees, D. J.; Baker, J.; Stewart, J. P.; Head-Gordon, M.; Gonzalez, C.; Pople, J. A. *Gaussian 94*, revision B.2; Gaussian, Inc.: Pittsburgh, PA, 1995.
(18) Pearson, R. G. *J. Chem. Educ.* **1987**, *64*, 561.
(19) Pearson, R. G. *Proc. Natl. Acad. Sci. U.S.A.* **1986**, *89*, 1827.
(20) Burdett, J. K.; Coddens, B. A. *Inorg. Chem.* **1988**, *27*, 3259.
(21) Passo, R. G. *J. Org. Chem.* **1989**, *54*, 1423.
(22) Faust, W. L. *Science* **1989**, *245*, 37.
(23) Zho, Z.; Parr, R. G. *J. Am. Chem. Soc.* **1989**, *11*, 7371.
(24) Schmidt, M. W.; Baldridge, K. K.; Boatz, J. A.; Elbert, S. T.; Gordon, M. S.; Jensen, J. H.; Koseki, S.; Matsunaga, N.; Nguyen, K. A.; Su, S.; Windus, T. L.; Dupuis, M.; Montogomery, J. A., Jr. *J. Comput. Chem.* **1993**, *14*, 1347.
(25) *Spartan*, version 4.1; Wavefunction Inc.: Irvine, CA, 1995.
(26) Rey, I. Ph.D. Thesis, University Bordeaux I, France, 1997.
(27) Zak, Z.; Ruzicka, A.; Michot, Ch. *Z. Kristallogr.* **1998**, *213*, 217.
(28) Haas, A.; Klare, Ch.; Betz, P.; Bruckmann, J.; Krüger, C.; Tsay, Y.-H.; Aubke, F. *Inorg. Chem.* **1996**, *35*, 1918.
(29) Benrabah, D.; Arnaud, R.; Sanchez, J.-Y. *Electrochim. Acta* **1995**, *40*, 2437.
(30) Berthier, C.; Gorecki, W.; Minier, M.; Armand, M. B.; Chabagno, J. M.; Rigaud, P. *Solid State Ionics* **1983**, *11*, 91.
(31) Abbrent, S.; Lindgren, J.; Tegenfeldt, J.; Wendsjö, Å. *Electrochim. Acta* **1998**, *43*, 1185.
(32) Burden, A. G.; Collier, G.; Shorter, J. *J. Chem. Soc., Perkin. Trans.* **1976**, *2*, 1627.
(33) Bernson, A.; Lindgren, J. *Polymer* **1994**, *35*, 4848.
(34) Pearson, R. G. *Chemical Hardness*; Wiley-VCH: Weinheim, 1997; p 55.